SUPPLEMENTAL FIGURES

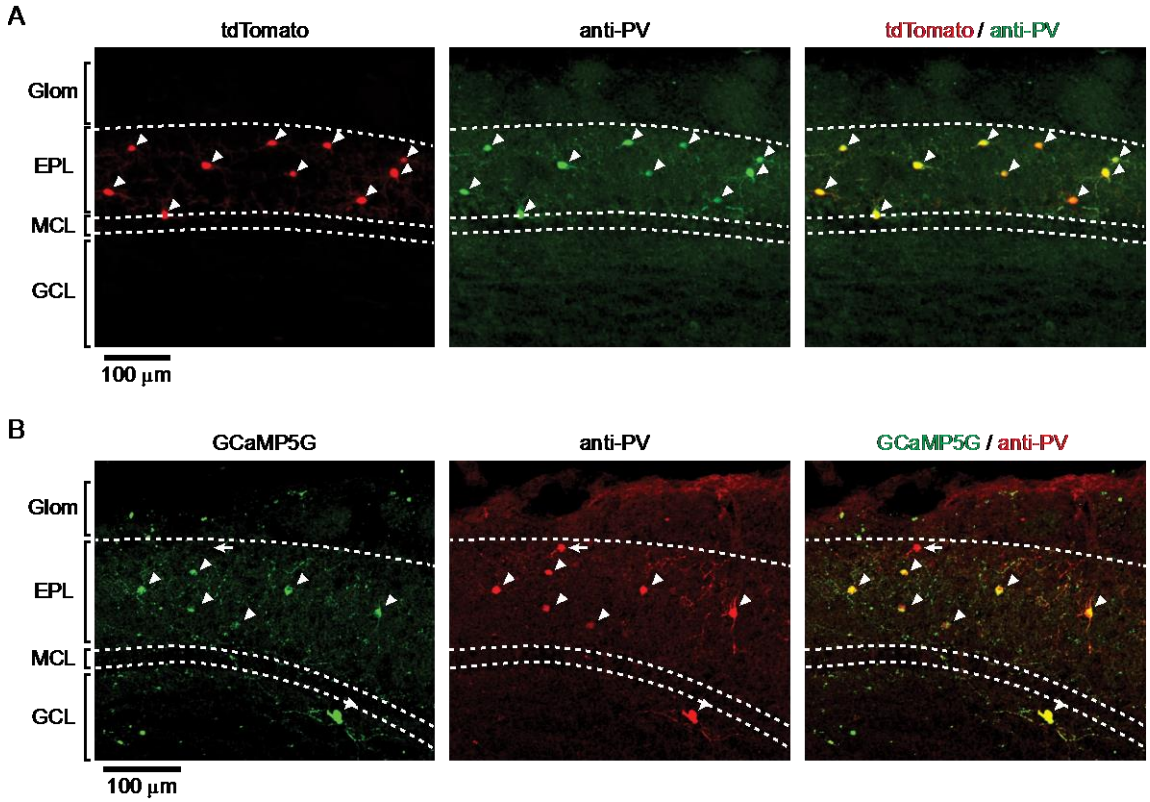

Figure S1. Validation of *PV-Cre* mouse line. (Related to Figure 1)

(A) Parasagittal section from a *PV-Cre* x *Rosa-LSL-tdTom* mouse. Left: tdTomato fluorescence. Middle: anti-PV immunostaining. Right: merged image showing the co-localization of tdTomato (red) and PV (green). 96% of PV-positive cells expressed tdTomato (1163 out of 1213 cells), and 96% of tdTomato-positive cells were PV-positive (1163 out of 1209 cells). tdTomato-expressing cells were concentrated in EPL (glomerular layer: 0.8%, EPL: 91%, mitral cell layer: 1.6%, internal plexiform layer: 3.3%, granule cell layer: 2.7%). Arrowheads: cells co-expressing tdTomato and PV. **(B)** Parasagittal section from a *PV-Cre* mouse injected with flex-GCaMP5G virus. Left: GCaMP5G fluorescence. Middle: anti-PV immunostaining. Right: merged image showing the co-localization of GCaMP5G (green) and PV (red). Within the densely infected area (typically 500-800 µm wide), 93% of PV-positive cells expressed GCaMP5G (94 out of 101 cells), and 99% of GCaMP5G-positive cells were PV-positive (94 out of 95 cells). GCaMP5G-expressing cells were concentrated in EPL (glomerular layer: 2.1%, EPL: 82%, mitral cell layer:

1.1%, internal plexiform layer: 8.4%, granule cell layer: 6.3%), consistent with the distribution of PV cells. Arrowheads: cells co-expressing GCaMP5G and PV, arrow: a cell which expresses only PV. Glom: Glomerular layer, EPL: external plexiform layer, MCL: mitral cell layer, GCL: granule cell layer. Dotted lines represent the borders between layers.

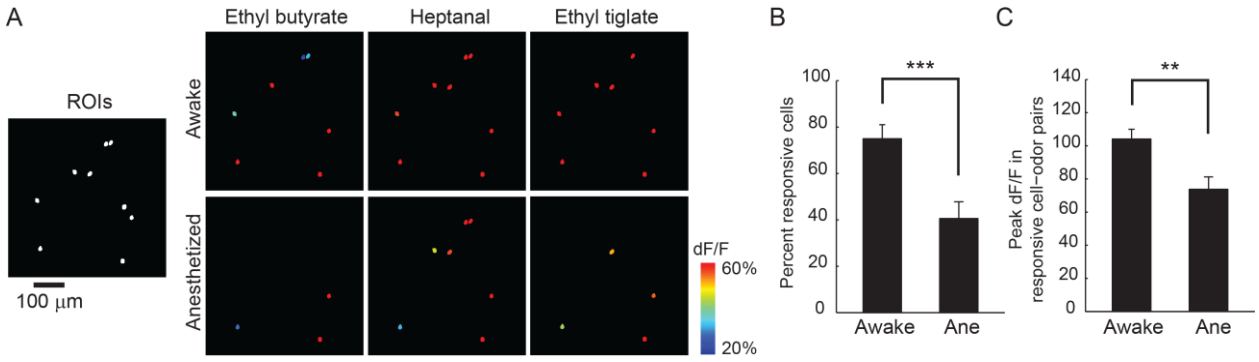

Figure S2. Odor-evoked responses in PV cells are attenuated by anesthesia. (Related to Figure 3)

(A) Odor-evoked activity maps of the same PV cells (pseudocoloring represents odor-evoked GCaMP5G dF/F response averaged across seven trials) recorded before and after the induction of urethane (1.5g/kg) anesthesia. PV cells respond more strongly to the same odors in the awake state (top) compared to the anesthetized state (bottom). The left panel shows all imaged PV cells in white. **(B)** Summary data showing the fraction of responsive cells to each odor in the awake and anesthetized state (average and SEM, n = 3 mice, 21 mouse-odor pairs). ***$p < 0.001$. (C) Summary data showing the peak response amplitudes of the responsive cell-odor pairs in the awake and anesthetized state (awake: 146 cell-odor pairs; anesthetized: 79 cell-odor pairs). **$p = 0.0012$.

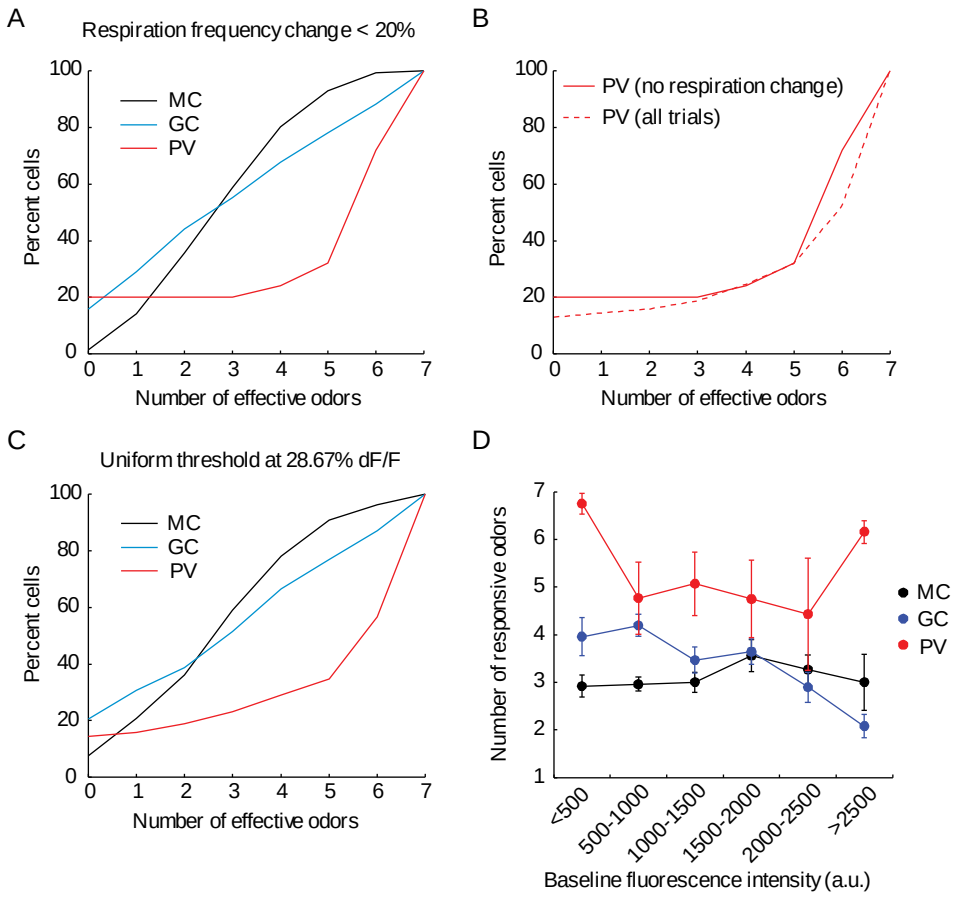

Figure S3. Broad odor tuning of PV cells does not reflect odor-evoked increases in respiration frequency, different detection thresholds across cell types, or expression levels of GCaMP5G. (Related to Figure 3)

(A) PV cells show broader tuning than mitral or granule cells even after rejecting trials in which respiration frequency changed during odor application. Cumulative frequency plot of odor tuning broadness (the number of odors eliciting responses out of the seven tested odors) calculated using only trials in which averaged respiration frequency during the odor period changed less than 20% from that during the baseline period. Black: mitral cells (n = 7 mice, 290 cells). Blue: granule cells (n = 3 mice, 375 cells). Red: PV cells (n = 5 mice, 69 cells). **(B)** The broadness of PV cell odor tuning is largely unaffected by removing trials in which respiration frequency increased by >20% during odor application. 65% of all the trials were rejected (181 out of 280 trials). Curves show the tuning broadness of PV cells with (red solid line, same as in (A)) or without (red dotted line, same as the red line in Figure 3D) the constraint on the respiration

frequency. **(C)** PV cells show broader tuning than mitral or granule cells even when the same threshold value (28.67% dF/F: the median value for all the cells included in the analysis shown in Figure 3D) was applied to all the cell types for detecting responsive cell-odor pairs. **(D)** PV cells show broader odor tuning than mitral or granule cells regardless of basal GCaMP5G fluorescence intensity in individual cells. Cells are sorted into bins based on the fluorescence intensity before odor application. All the data points for PV cells are above those for granule and mitral cells.

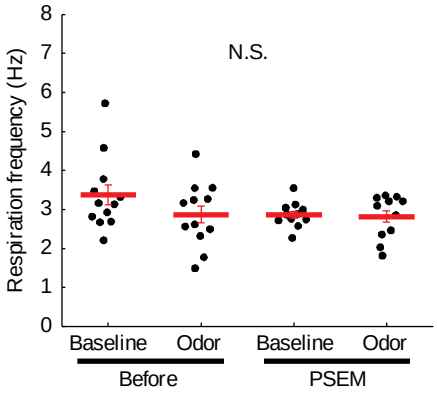

Figure S4. Neither PSEM nor odor application affects respiration frequency. (Related to Figure 5)

Average respiration frequencies were calculated for the mice in Figure 5 and Figure 6 for the following four conditions: 1) before PSEM application, baseline period (10-second period preceding odor application), 2) before PSEM application, odor period (4-second period of odor application), 3) after PSEM application, baseline period, and 4) after PSEM application, odor period. There is no significant effect of either PSEM or odor application on the respiration frequency (before vs PSEM: $p = 0.1975$; baseline vs odor: $p = 0.1873$; $n = 14$ mice, two-way ANOVA test).

SUPPLEMENTAL EXPERIMENTAL PROCEDURES

Immunohistochemistry

Olfactory bulb sections (30 μm) were cut using a frozen microtome and rabbit anti-parvalbumin (1:3000) (Yoshihara et al., 2005) staining was performed in the presence of 0.2 % triton. As a secondary antibody, either Alexa488- or Alexa594-conjugated goat anti-rabbit antibody (1:1000) (Invitrogen) was used. GCaMP5G expression was detected using the endogenous GCaMP5G fluorescence without amplification.

Slice preparation for electrophysiology

Mice (3-5 weeks old) were anesthetized with isoflurane and decapitated. OBs were removed and placed into ice cold artificial cerebrospinal fluid (aCSF) containing (in mM) 83 NaCl, 2.5 KCl_2, 0.5 $CaCl_2$, 3.3 $MgSO_4$, 1 NaH_2PO_4, 26.2 $NaHCO_3$, 22 glucose, and 72 sucrose, equilibrated with 95% O_2 and 5% CO_2. Coronal or horizontal slices (300-400 μm) were cut using a vibrating slicer and incubated at 35 °C for 30 minutes. Slices were transferred to a recording chamber and superfused with aCSF containing (in mM): 119 NaCl, 5 KCl, 2.5 $CaCl_2$, 1.3 $MgSO_4$, 1 NaH_2PO_4, 26.2 $NaHCO_3$ and 22 glucose, equilibrated with 95% O_2 and 5% CO_2. All experiments were conducted at 28–30 °C.

Data analysis

Lateral motion was corrected first by cross correlation-based image alignment (Turboreg (Thevenaz et al., 1998), ImageJ plugin). ROIs corresponding to individual cells were manually drawn and the pixels in each ROI were averaged to estimate the fluorescence of a single ROI. A background ROI was drawn close to each cell and the average pixel value of the background ROI was subtracted from the average pixel value of each ROI. The first application of each odor

was excluded from the analysis of odor tuning properties to avoid the influence from the increased sniffing to novel odors (Kato et al., 2012; Wesson et al., 2008). For each odor application, the trace was smoothed (30-frame window LOESS) and normalized by the baseline (for the odor application trials, the median value from 10 seconds before odor onset; for the spontaneous activity trials, the median value from the whole trace). The baseline fluctuation (σ) was estimated for each ROI by taking the median of standard deviations of baseline traces for all trials. Odor response was assessed over the ten seconds following odor onset. ROC analysis was used to determine the following thresholds for identifying responsive odor-ROI pairs yielding a 95% true positive rate; mitral cells: 1.9 x σ ; granule cells: 2.2 x σ ; PV cells: 2.3 x σ . Odor-ROI pair was considered responsive only when its response exceeds threshold for 15 successive image frames both 1) in at least half of all trials and 2) in the trial-average trace. For responsive odor-ROI pairs, Change Index (CI) on each trial (trial X) was defined as (response on trial X – the initial response) / (response on trial X + the initial response). We used the peak dF/F during the response period as response, and the peak was corrected for random fluctuations by subtracting 2.4168 x σ (the calculated theoretical value of the peak from normally-distributed random fluctuations of 284 image frames). Correlation coefficients between odor representations (Figure 3F) were calculated from population response vectors for seven different odors, each of which was made by concatenating the peak dF/F amplitudes during the odor detection periods (ten seconds after the odor onset) of all the cells across all mice.